



# Recent Advances in Active Metal Brazing of Ceramics and Process

S. Mishra<sup>1</sup> · A. Sharma<sup>2</sup> · D. H. Jung<sup>1</sup> · J. P. Jung<sup>1</sup>

Received: 9 August 2019 / Accepted: 5 November 2019 / Published online: 14 November 2019  
© The Korean Institute of Metals and Materials 2019

## Abstract

Ceramic to metal joining has its potential applications in microelectronics packaging, metal–ceramic seals, vacuum tubes, sapphire metal windows, etc. But there are many limitations in joining this duo of materials that range from their structures, nature of bonding, physical properties to a complex phenomenon like wetting, spreading and adhesion. The current review discusses these critical issues from the aspects of thermodynamics, the role, and type of active elements, Ag–Cu–Ti brazing filler system and the reliability factors like residual stress, coefficient of thermal expansion, material reliability, pores and unbonded regions on the surface which affect the mechanical reliability of the joint.

**Keywords** Ceramic · Metal · Active metal brazing · Wetting · Reliability

## 1 Introduction

Both ceramics and metals are widely used engineering materials. Ceramics are brittle in nature with its strength almost two-third of its theoretical strength. They are lightweight, hard, stable at high temperature, brittle and have low fracture toughness [1]. On the other hand, most metals are soft, ductile with better fracture toughness and have less strength compared to ceramics [2]. To combine the functional properties of ceramics and make up for its brittleness and low fracture toughness, it is required to join them with metals which require application in industries like electronics, electrical and especially in microelectronics packaging [3]. A welding/brazing process requires that base metals to arrange in a stable configuration which results in interatomic or intermolecular forces between the different joining atoms under the application of heat and pressure [4]. Theoretically, it is impossible to bond metals and ceramics because of their inherent different electronic structures and bonding type i.e. ionic or covalent for ceramics and dominantly metallic in case of metals [4]. Due to the advancement of materials

science, various high end spacecraft, automobiles and packaging devices needs to bond with ceramics for diverse applications. Therefore, there is a great need to study the ceramic and metal contact surfaces and various processes that affect their bonding. This review paper focusses on the various techniques for brazing and applications. We have also overviewed the mechanism of metal–ceramic bonding and further directions in this field to improve the joints. A brief gamut of metal–ceramic joining process is given in below Fig. 1 [5].

Out of these, active metal brazing will be our topic of interest for the rest of this review article. For example, the authors bonded the zirconia and titanium using the active metal brazing method, which has sound brazing joint. In addition, many pieces of research have been done to improve the joint strength at low brazing temperature [6]. Furthermore, the authors evaluated a compressive strength of the ZrO<sub>2</sub>/Ti–6Al–4V joint brazed using the active metal filler Ag–Cu–Sn–Ti. The active brazing was conducted at a 750 °C for 30 min in a vacuum furnace. The average compressive strengths of five samples were 1477 MPa, which means a favorable joint strength [7]. Additionally, the authors reported a maximum shear strength of 15 MPa for Cu/Al<sub>2</sub>O<sub>3</sub> joint when brazed with AgCuTiSn filler metal [8].

Apart from many, some of the greatest advantages of the brazing process are that it minimizes the component distortion, base material dissolution is low, and it can be used to join dissimilar materials like metals and ceramics which is not achieved in case of welding. A major limitation of

✉ J. P. Jung  
jppjung@uos.ac.kr

<sup>1</sup> Department of Materials Science and Engineering,  
University of Seoul, Seoul 02504, Republic of Korea

<sup>2</sup> Department of Materials Science and Engineering  
and Department of Energy Systems Research, Ajou  
University, Suwon 16499, Republic of Korea

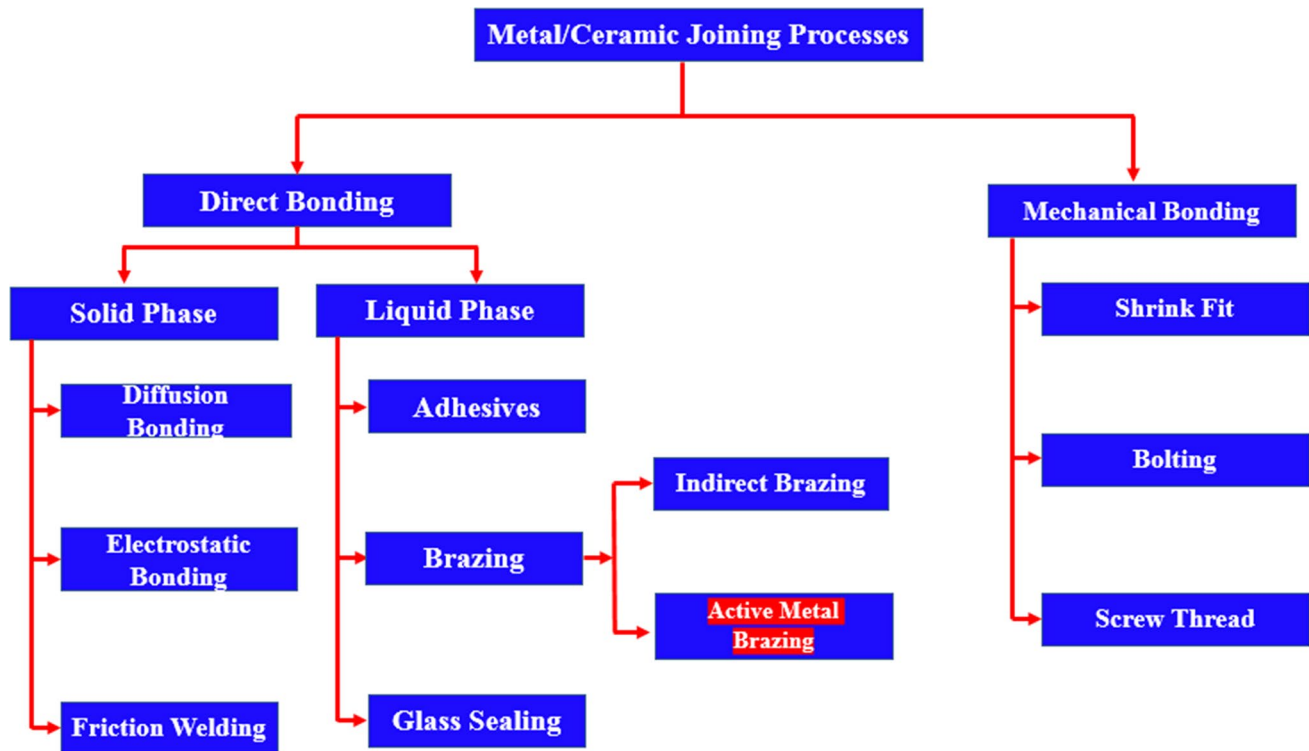


Fig. 1 Metal to ceramic joining processes

ceramic to metal brazing is the poor wetting of liquid metal on ceramics which restricts the spreading and adhesion. Other than this, the high-temperature instability and poor strength of the brazed joint is a limitation because of the low melting point of the filler metal [9].

## 2 Wetting and Spreading Theory

Authors reviewed the effect of various factors on brazing technology and mentioned that principal requirements of a brazing process are that the filler metal should wet and spread well over the faying surfaces [10]. The wetting and spreading behavior of the liquid metal on the ceramic surface is important in determining the strength and adhesion of the joint between ceramic and metal. Surface and interfacial interactions between the solid and liquid play a vital part in ascertaining the extent of wetting and spreading. There are various forces like Vander Waals, electrostatic and molecular forces which play an important role in wetting. These forces act at various length scales and have been examined with techniques like surface force apparatus, atomic force microscopy, and molecular dynamics. [11–13]

Thomas Young in 1805 formulated an equation for a clean, homogeneous and flat solid surface. He related the interfacial energy  $\gamma_{ij}$  and surface tension, where the subscripts *i* and *j* refers to vapor (*v*), liquid (*l*) and solid (*s*), the

equilibrium contact angle  $\theta$ , through Young's equation, the figure for which is mentioned below:

$$\gamma_{sv} - \gamma_{sl} = \gamma_{lv} \cos \theta \quad (1)$$

$\gamma_{sv}$  and  $\gamma_{lv}$  are the surface tension or cohesion forces of the condensed phase which pulls the surface atoms towards the bulk and  $\gamma_{sl}$  is the interfacial energy of solid–liquid interface.

For spreading of liquids on a solid, a spreading parameter *S* is defined as

$$S = \gamma_{sv} - \gamma_{sl} - \gamma_{ls} \quad (2)$$

If  $S > 0$ , spreading occurs completely to minimize the surface energy.

If  $S < 0$ , the liquid droplet settles like a lens on top of the solid-like (Fig. 2).

Wenzel in 1936, introduced the concept of surface roughness as the solid surfaces generally are not ideally smooth and fabrication process introduces some pores, striations, microgrooves or irregular convex. He introduced a parameter known as roughness (*r*) and modified Young's equation as

$$\cos \theta_w = r \cdot \cos \theta \quad (3)$$

$\theta_w$  is the wetting angle considering the surface roughness (*r*) which is the roughness factor and is the quotient of the actual surface area to the geometric surface area. For rough surfaces, the value of *r* is greater than 1. According to his

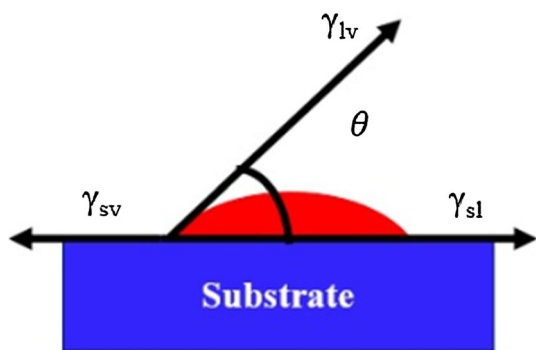


Fig. 2 Schematic of a liquid droplet over a solid substrate

model, the liquid is in contact and interacts with the entire solid and penetrates the capillaries completely under the action of capillary forces. Also, defects present on solid surfaces can pin the triple-phase boundary which can affect the phenomenon like wetting and spreading [14]. If a further liquid is added under this condition, the liquid drop will be inflated, there will be a rise in the equilibrium contact angle until the threshold value of the contact angle will be achieved. This angle is known as the advancing contact angle ( $\theta_{Ad}$ ). Likewise, if there is a deflation of the droplet, the corresponding angle drops until the droplet recedes and is called as  $\theta_{rec}$ . The difference between these contact angles ( $\theta_{Ad} - \theta_{rec}$ ) is called contact angle hysteresis. This contact angle hysteresis arises a force which is given by [11, 15–17]

$$F = \gamma(\cos\theta_{Ad} - \cos\theta_{rec}) \tag{4}$$

### 3 Problems in Wetting of Ceramics Substrate by Liquid Metal

Whether wetting happens or not and its extent is influenced by the surface tensions and the reactivity of the ceramic and corresponding liquid metal [18–20]. Generally, liquid metals do not wet the ceramic substrate unless there is a reaction between the corresponding ceramic–metal interface which increases the wetting of the liquid metal. Surface properties of the ceramic, its microstructure and reactivity of the brazing filler metal with the ceramic under the brazing ambience decides the extent of wetting [20]. To achieve higher wetting and good adhesion, an active element is added into the brazing filler metal for bonding the ceramic to metal. The spreadability of the filler metal onto the substrate can be determined by the spread area difference of the melt before and after the heating. The spreadability is defined from the following relation [21–29]:

$$S = \frac{D - H}{D} \times 100 \tag{5}$$

where H is the vertical distance between the top to bottom and D is the diameter of the molten filler metal (assuming it to maintain a spherical shape). In addition,  $D = 1.43 \rho^{1/3}$ , where  $\rho$  is the filler material density. The solid–liquid work of adhesion follows from the Young–Dupre equation:

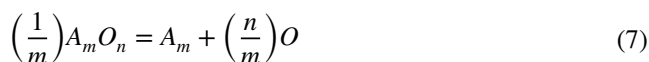
$$W_{sl} = \gamma_{sv} + \gamma_{sl} - \gamma_{ls} = \gamma_{ls}(1 + \cos \theta) \tag{6}$$

The details and type of such active elements and their effects will be discussed in later portions of this review.

### 4 Reactive Wetting

There is a possibility of reducing the contact angle in non-reactive systems by introducing an active element into the filler alloy which can induce chemical reaction at the interface and enhance the wetting properties [30]. These elements promote the wetting by lowering the surface tensions of the liquid or by enhancing the segregation of oxygen to the ceramic–metal interface.

Consider an oxide  $A_mO_n$  dissolving to metal M under the addition of reactive element Re. The dissolution reaction is [31]:



The oxygen molar content in the dissolution melt  $x_o^D$  is given by

$$x_o^D = \left(\frac{n}{m}\right)^{\frac{m}{m+n}} \cdot K_D^1(T)^{\frac{m}{m+n}} \cdot \exp\left(-\frac{n}{m+n} \epsilon_o^{Re} \cdot x_{Re}\right) \tag{8}$$

where  $\epsilon_o^{Re}$  is the Wagner first-order interaction coefficient between O and Re in liquid M.

$\epsilon_o^{Re} < 0$ , the dissolution of oxygen in the M-Re in equilibrium with oxide  $A_mO_n$  increases rapidly as the amount of Re increases.

$\epsilon_o^{Re} \ll 0$ , precipitation of  $Re_yO_z$  can be promoted by the reaction:



$$K_p(T) = \{x_{Re}\gamma_{Re}\}^y \cdot \{x_o\gamma_o^\infty\}^z = \exp\left(\frac{\Delta^\circ G_f^{Re_yO_z}}{RT}\right) \tag{10}$$

The mole fraction of oxygen dissolved in liquid metal M in equilibrium with reaction product  $Re_yO_z$  is given by:

$$x_o^P = K_p'(T)x_{Re}^{-\frac{y}{z}} \exp(-\epsilon_{z'}^o x_{Re}) \tag{11}$$

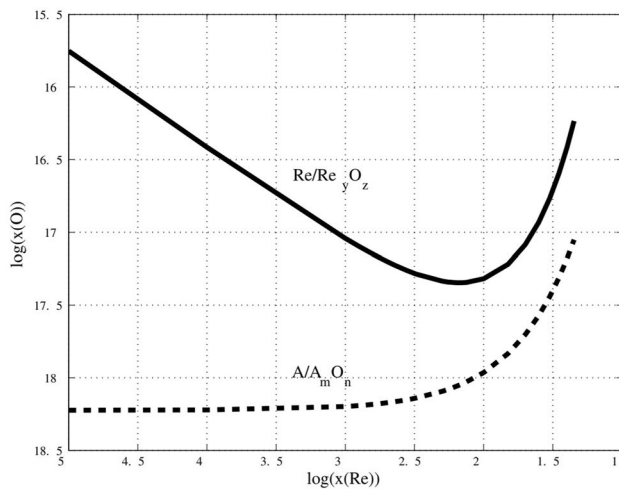


Fig. 3 Slightly reactive element addition [31]

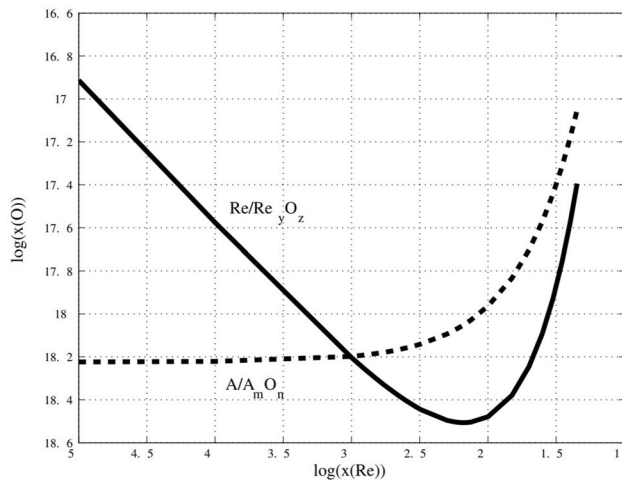


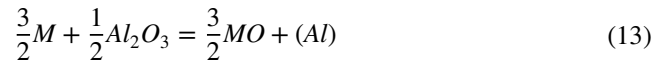
Fig. 4 Highly reactive element addition [31]

$$K_P^p(T) = K_P(T)^{1/z} \cdot \gamma_{\text{Re}}^{y/z} \cdot (\gamma_o^\infty)^{-1} \quad (12)$$

It is evident from the above Figs. 3 and 4 that the ceramic dissolution increases as the reactive element addition increases in both cases. In case 2 (Fig. 4), a more reactive element is added and has a strong affinity for oxygen as  $\epsilon_o^{\text{Re}} \ll 0$  and as a result the precipitation of  $\text{Re}_y\text{O}_z$  which is illustrated by the intersection of  $A/A_m\text{O}_n$  and  $\text{Re}/\text{Re}_y\text{O}_z$  equilibrium curves but this is not the case when a less reactive element is added and  $\text{Re}_y\text{O}_z$  does not precipitate (Fig. 3). The more reactive element as in Fig. 4 forms a precipitate and it will decrease the contact angle considerably if the precipitation product is wettable [31].

## 5 Thermodynamic Considerations of Metal–Ceramic Interface

Consider a metal and ceramic (alumina) reaction as below:



The degree of dissolution is determined by the equilibrium concentration of Al in liquid M coming from the dissolution of  $\text{Al}_2\text{O}_3$ . It is equal to the difference in the final and initial mole fraction of Al,  $X_{\text{Al}}$ . In case  $X_{\text{Al}} \ll 1$ , the equilibrium mole fraction of Al is written as:

$$X_{\text{Al}} = \exp\left(\frac{-\Delta G_r^*}{RT}\right) \quad (14)$$

$\Delta G_r^*/RT$  is an approximate measure of relative reactivity of different systems [9].

The mechanical strength of a metal–ceramic interface cannot just be evaluated by the adhesion energy but also by the bulk mechanical state of the materials like the residual elastic or plastic energy stored in the material [32].

The thermodynamic driving force for a ceramic to metal joint/interface is the change in free energy which occurs when an interface is formed as a result of intimate contact between the two materials [31]. This free energy change per unit area is given by:

$$\Delta G^{\text{inf}} = \sigma_{\text{sv}} + \sigma_{\text{lv}} - \sigma_{\text{sl}} \quad (15)$$

$\Delta G^{\text{inf}}$  is the change in Gibbs free energy due to the creation of an interface between ceramic and the metal.  $\sigma_{\text{sv}}$  and  $\sigma_{\text{lv}}$  are the surface energies of the solid and liquid and  $\sigma_{\text{sl}}$  is the solid–liquid interfacial energy. If only a chemical reaction has resulted in a chemical bond between the materials forming an interface, the change in free energy  $\Delta G^{\text{inf}}$  equals the work of adhesion  $W_{\text{ad}}$ . Work of adhesion is defined as the work done in separating the interfacial joint and taking the original surfaces to infinity. Hence,

$$W_{\text{ad}} = \sigma_{\text{sv}} + \sigma_{\text{lv}} - \sigma_{\text{sl}} \quad (16)$$

Higher the  $W_{\text{ad}}$ , stabler is the solid–liquid interface. Under equilibrium conditions, an equilibrium between the surface and interfacial energies is quantified by Eq. (1) and from (1) to (6), it can be deduced that [18]

$$W_{\text{ad}} = \sigma_{\text{lv}}(1 + \cos \theta) \quad (17)$$

The contact angle between metallic and ceramic oxide was measured by Eustathopoulos and coworkers by sessile drop technique. They calculated the oxygen molar fraction in the liquid metal  $x_o^{\text{D}}$  using the homologous thermodynamic properties for the oxides and thermodynamic properties for the oxides and estimated values of activity coefficients of

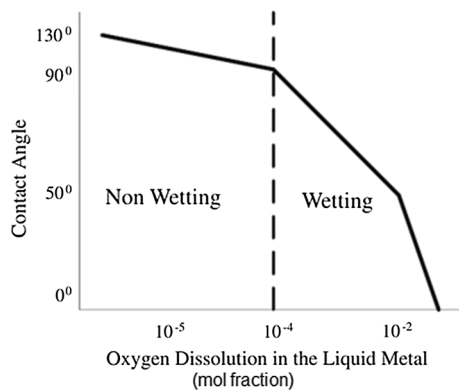


**Fig. 5** Schematic of the contact angle as a function of oxide dissolution content [31]

both oxygen and ceramic cation in the melt. He found out a relationship between oxide dissolution extent  $x_0^D$  and the contact angle at the ceramic–metal junction. His findings are briefed in the below Fig. 5.

The limiting value of  $x_0^D$  for wetting and nonwetting between oxide ceramic and metal is around  $10^{-5}$ . The effects of the furnace atmosphere on the chemistry of the liquid metal was not considered while calculating the extents of dissolution [31].

## 6 Active Metal Brazing

Active metal brazing is a joining method where ceramics can be joined to metals or itself through a brazing alloy known as active brazing alloy (ABA) under the application of heat and pressure. Usually, ABA contains an active element whose role is to form the reaction products with ceramic and metal and enhance the wetting, adhesion, and bonding which is difficult in case of metal to ceramic without the application of active element. The bonding and adhesion are achieved by ABA such that the brittle phase fraction is optimized to provide strength to the joint at the same time not to embrittle it [33]. Below Fig. 6 [34] is a macroscopic image of the  $ZrO_2$  and Ti–6Al–4V joined through active metal brazing by authors.

### 6.1 Types of Active Metals

Active elements are generally added to filler alloy to increase the wetting. First-class of active elements are metals like Ti, Sc, Zr, Cr and are one of the most effective added elements. These elements enhance wetting for ionic as well as covalent bonds. [35].

Amongst non-metals are elements like O, Cl, S, Se. These elements improve the wetting of metals like Cu, Ni, Ag, Pb, etc. on the solids which have ionic chemical bonds in

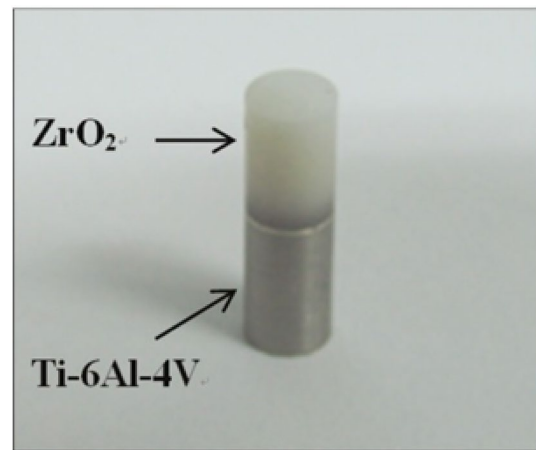


**Fig. 6**  $ZrO_2$ -Ti alloy brazing sample [34]

compounds like oxides, sulfides, etc. The reason for wetting being the highly electronegative element takes the electron of solvent metal atoms and leaves them positively charged ions which have high coulombic interaction with oxygen anions and thus improves the wetting. Example being fluorides, copper oxides, and other ionic compounds. Oxygen has specific efficacy in case of Ag–Cu alloys [35].

Following Fig. 7 [35] represent the effect of the Ti concentration on the contact angle of nitride ceramics surface. The contact angle is seen to decrease with increasing active metal content for different concentration of Cu–Ga melts (1–3) as mentioned in Fig. 7 [35].

Below mentioned Fig. 8 [35] represents and compares the effect of the same Ti and Zr content on Zirconia ceramics by Cu–Ga melts at 1150 °C. Zr, in this case, is more effective than Ti as shown in Fig. 8 [35].

The Table 1 mentions and compares the wetting angle of cubic boron nitride by different metal melts at different temperatures:

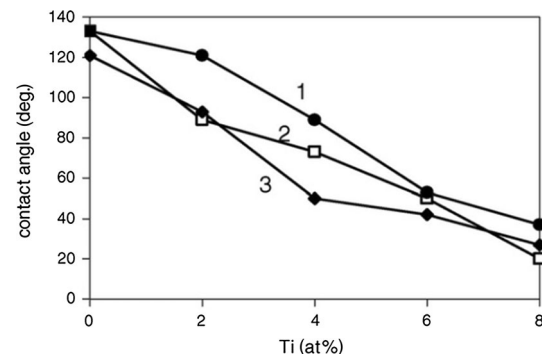


**Fig. 7** Influence of Ti on wettability of nitride ceramics by Cu–Ga melts at 1150 °C (1 and 2) and 1100 °C (3):(1) (Cu–10%Ga)/ $Si_3N_4$ ; (2) (Cu–20%Ga)/ $Si_3N_4$ ; (3) (Cu–17.5% Ga)/AlN [35]

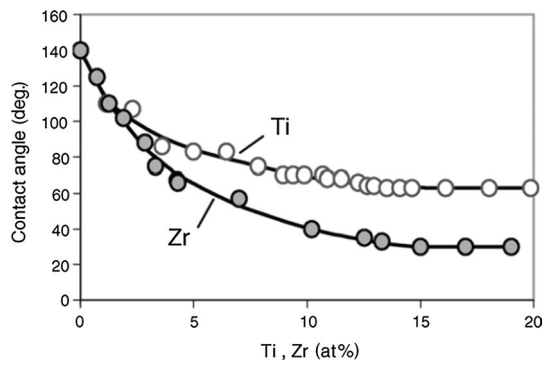


**Fig. 8** Influence of Ti and Zr on the wettability of zirconia by Cu–Ga melts at 1150 °C [35]

**Table 1** Comparison of the wetting angle of cubic boron nitride by different metal melts at different temperatures [35]

Melt at%	Temperature (°C)	Contact angle (°)
Cu	1100	137
Ag	1000	146
Sn	1100	137
Cu + 10%Sn	950	136
Cu + 20%Sn	950	135
Cu + 10%Sn + 15%Ti	950	28
Cu + 20%Sn + 15%Ti	950	21

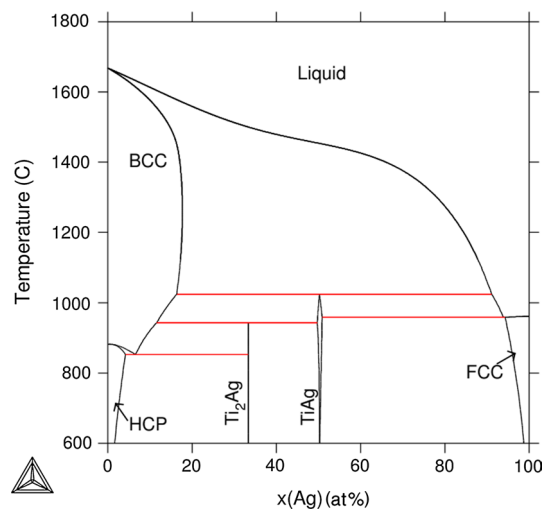


**Fig. 9** Calculated phase diagram between Ag–Ti [36]

## 6.2 Popular Ag–Cu–Ti Brazing System

Though there are many brazing alloy systems, the scope of this article is limited to AgCuTi discussion only. AgTi

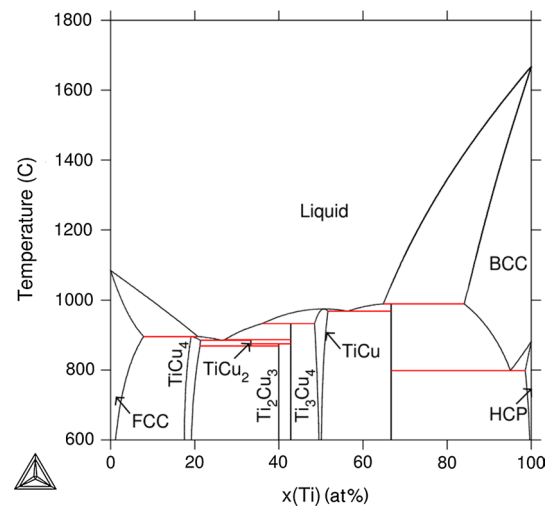


**Fig. 10** Calculated phase diagram between Cu–Ti [36]

system has two intermetallic compounds as shown in Fig. 9 [36] having peritectic decomposition  $Ti_2Ag$  and  $TiAg$  while  $CuTi$  has 6 intermetallic phases as in Fig. 10 [36] and one out of them melts congruently.

The ternary system of  $AgCuTi$  has two features. The first one is the continuous solid solution between  $Ti_2Cu$  and  $Ti_2Ag$  and the second one is the miscibility gap between Ti-rich and Ag rich liquids. The liquidus temperature is quite low for Ag–Cu eutectic and these alloys are used for low-temperature brazing of ceramic to metal under the temperature range 800–900 °C.

Ag presence considerably increases the activity of Ti which ultimately enhances the interfacial reactions with the ceramic materials [30, 37]. The enhanced activity of Ti causes it to react and form compounds with partially metallic character thus improving the wettability [38, 39].

Below mentioned Fig. 11 [8] shows the SEM microstructure of the bonding interface of  $Cu-Al_2O_3$  through  $AgCuTiSn$  filler metal. There are Ag rich and Cu rich phases along with some reaction products.

A detailed knowledge of the various reaction phases forming in  $AgCuTi$  system in the temperature range 800–900 °C is necessary to understand the reactive wetting and develop brazing joints with good brazing strengths. Experimental study of the  $AgCuTi$  system was done by Eremenko et al. [40–42], critically assessed by Chang et al. [43] and Kubachewski et al. [44]. Eremenko reported in his studies that the liquid miscibility gap in the liquid separated into Ti-rich and Ag rich solutions. There are no ternary compounds in  $AgCuTi$  system and the data for the  $AgTi$  and  $CuTi$  system has been given in the below-mentioned Table 2 [43].

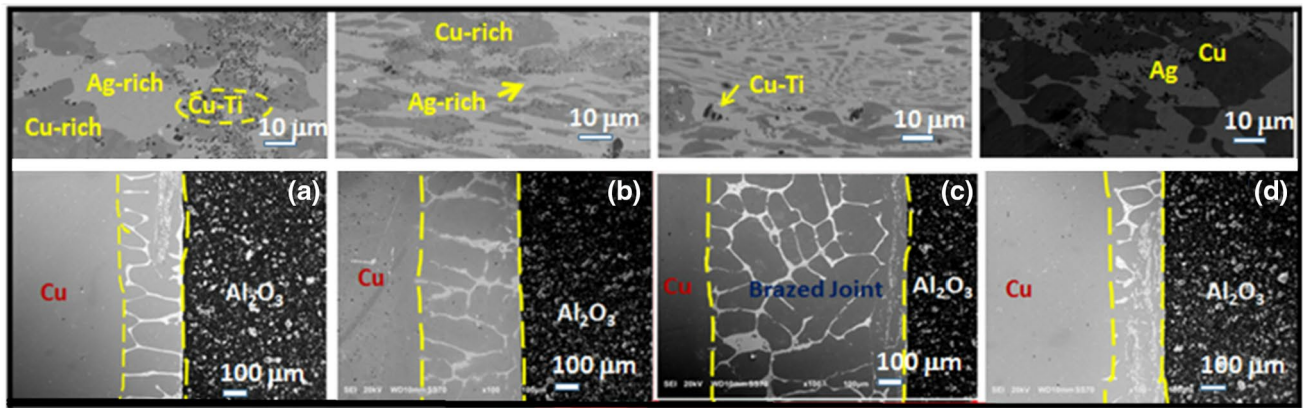


**Fig. 11** SEM microstructure of the joint between  $\text{Al}_2\text{O}_3$ -Cu bonded through AgCuTiSn filler [8]

**Table 2** Symbols and crystal structures of stable phases in AgCuTi system [44]

Structure report	Diagram symbol	Symbol used in thermo- data file	Pearson symbol/space group/prototype	Lattice parameter
A <sub>1</sub>	(Ag)	FCC_A1	cF4	a = 408.57
	(Cu)	Fm3m	Cu	a = 361.46
A <sub>3</sub>	$\alpha$ -Ti	HCP_A3	hP2	a = 330.65
A <sub>2</sub>	$\beta$ -Ti	BCC_A2	p6 <sub>3</sub> /mmc	Mg
			cI2	Im3m
	TiCu <sub>4</sub>	TiCu <sub>4</sub>	oP20	a = 452.5
			Pnma	b = 434.1
	TiCu <sub>2</sub>	TiCu <sub>2</sub>	ZrAu <sub>4</sub>	c = 1295.3
			oC12	a = 436.3
	Ti <sub>2</sub> Cu <sub>3</sub>	Ti <sub>2</sub> Cu <sub>3</sub>	Amm2	b = 797.7
			VAu <sub>2</sub>	c = 447.3
	Ti <sub>3</sub> Cu <sub>4</sub>	Ti <sub>3</sub> Cu <sub>4</sub>	tP10	
			P4/nmm	c = 1395
C11 <sub>b</sub>	Ti <sub>2</sub> Cu	Ti <sub>2</sub> M	Ti <sub>2</sub> Cu <sub>3</sub>	
			tI14	a = 313
	Ti <sub>2</sub> Ag	TiM	Ti <sub>3</sub> Cu <sub>4</sub> Ti	c = 1994
			tI6	a = 295.3
B11	Ti <sub>2</sub> Cu	TiM	I4/mmm	c = 1073.4
			MoSi <sub>2</sub>	a = 295.2
	TiAg	TiM		c = 1185
			tP4	a = 290.3
	TiCu	TiM	P4/mmm	c = 574
			TiCu	a = 310.8–311.8 c = 588.7–592.1

## 7 Joint Reliability and Possible Solutions in Metal–Ceramic Brazing

### 7.1 Factors Influencing Metal–Ceramic Joint Reliability

Joining metals to ceramics is a difficult task because of the difference in the inherent physical and chemical nature of metal and ceramics [45, 46]. The schematic in Fig. 12 states the various causes for scattering in the joint strength.

At the micron scale, the interface contacts formed during wetting, physical and chemical reaction is of importance from a reliability perspective [47]. Other key factors influencing the joint reliability are the cracks in the interface and the thermal and residual stresses. High magnitudes of thermal stress while joining and in-service conditions introduce flaws into the joint. The distribution of weakly or unbonded interface results in a substantial reduction in joint strength [48, 49].

When cooled from the bonded temperature, the development of residual stresses is a major disadvantage and limitation to the ceramic–metal joint as these can severely reduce the strength and sometimes lead to catastrophic failure [50]. The mechanical characterization of the ceramic–metal joint is complex, and some characteristics outweigh others in certain applications [51]. The subsequent section will be focused on reliability issues related to joining researches and the factors affecting the reliability of metal–ceramic joint.

#### 7.1.1 Material Reliability Issues

Ceramic is the crucial material for achieving sound mechanical joints due to its brittleness [52]. When the bulk properties of the ceramic material are not enough, it fractures in a brittle manner in the presence of thermal stresses. These materials are produced by different forming methods followed by sintering at high temperature. Diamond cutting tools and abrasives are required for shaping complicated shapes because of their high hardness and brittleness. At the same time, sharp edges and corners must be avoided

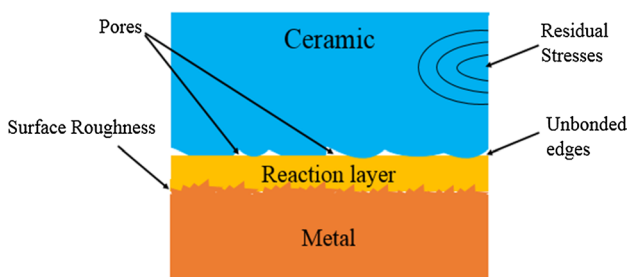


Fig. 12 Schematic of factors influencing metal/ceramic joint

to prevent stress concentration [53]. Microcracks are created into the surface when the ceramics are grounded by the metal-bonded diamond wheel. Microcrack size is based on the diamond grit size of the wheel and on the material removal rate also. Surface damage caused by these microcracks can create major cracks in the ceramic and lead to unreliable joints. Hence, the ceramic surface must be free from such cracks to avoid the possibility of poor joints.

This can be achieved by utilizing sintered ceramic. Most ceramic parts over 2 cm in size must be grounded as the distortion of the parts during sintering requires grinding for dimensional control of sintered ceramic. Further operations like re-sintering or lapping are needed to obtain defect-free surfaces. In the case of re-sintering, the damaged layer is repaired through sintering while the same is removed physically in the lapping operation. It is a requirement that the thickness eliminated through lapping process must remove the damaged layer completely [52].

#### 7.1.2 Thermal Expansion and Residual Stress

Residual stress is the stress that remains in the material when the initial cause of the stress is removed. Thermal stresses usually occur in a rigidly constrained material that is heated and in a material with temperature gradients. Thermal residual stresses play a key role in various mechanical behavior and joint strength. There are three classifications for residual thermal stresses based on the mechanism which produces them, Firstly, volumetric change i.e. expansion or shrinkage caused by phase transformation through temperature variation across the critical value. Secondly, the stresses induced by the difference in CTE values of the base materials at a stable or altering temperature. Thirdly, the thermal stresses as a result of temperature gradients causing differential thermal rates within the volume of material or structure and can possibly cause the cracking. Temperature change and the gradient is a necessary condition for these stresses to result from differential rates of contraction or expansion, but the temperature may or may not exist. Thermally-induced stresses from this source persist irrespective of temperature gradient [54]. Residual stress significantly affects the mechanical reliability of the interface as it may cause cracking on the ceramic side and plastic deformation on the metal side thus compromising the mechanical strength of the joint.

The residual stresses generated in the ceramic–metal joint for fully elastic conditions can be calculated by the following formula [55]:

$$\sigma_c = \frac{\Delta\alpha \cdot \Delta T \cdot E_m \cdot E_c}{E_m + E_c} \quad (18)$$

$\sigma_c$  is the residual stress after the joined has cooled to the room temperature,  $\Delta\alpha$  is the difference in thermal expansion



coefficient between materials,  $\Delta T$  is the difference in the temperature between joining and room temperature,  $E_m$  is Young’s modulus of metal,  $E_c$  is Young’s modulus of ceramic. Under the conditions of linear elastic linear plastic and in case of thermal stresses in metal exceeding its yield strength ( $\sigma_y$ ), the residual stress in the joint can be estimated by:

$$\sigma_c = \sigma_y + \Delta\alpha \cdot \Delta T \cdot E_{mp} \tag{19}$$

$E_{mp}$  is the linear strain hardening coefficient and  $\sigma_y$  is the yield strength of the metal. There is a non-uniform spread of residual stresses in the joint and along with the interface and its effect intensifies as it approaches nearer to the interface. Tensile stress is most detrimental in the interface and the ceramic, its direction is perpendicular to the interface and surface direction resulting in crack opening and hence fracture. The shape and dimensions of the metal/ceramic interface determine the breadth of the residual stress [56]. Sometimes it turns out that some specimen will be strong while others not despite being of the same kind and its due to the distribution and presence of cracks in the region of thermal stresses [56, 57].

Hadian proposed two methods to relieve thermal stresses. The first method is to insert a metal with a matching coefficient of thermal expansion and the other is to using a ductile metal which gets plastically deformed to relieve the thermal stress or a combination of both methods may also be used [58].

Through above Figs. 13 and 14, it is inferred that if the CTE of ceramic is less than CTE of metal, edge cracks are developed while core cracks are developed when the CTE ceramic is greater than CTE metal [59]. Zhou [55] recommended the following points: (1) low yield soft filler metals with low yield could release the residual stress. (2) Soft layer usage can reduce the residual stress by elastic or plastic

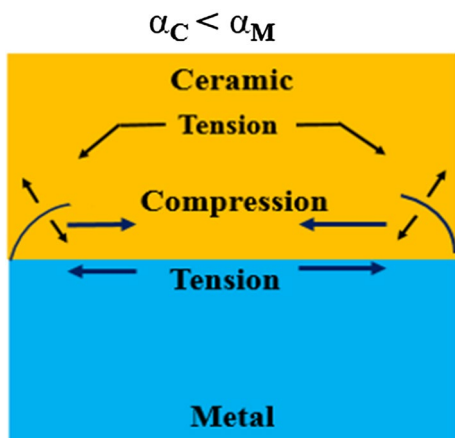


Fig. 13 Edge cracks in ceramics [58, 59]

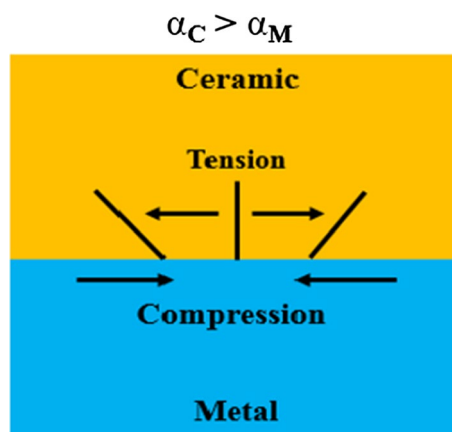


Fig. 14 Core cracks in ceramics [58, 59]

deformation of the interlayer, e.g., Applying Al or Cu as an interlayer. As per Eq. (16), residual stress will decrease with decreasing the Young’s Modulus. (3) Hard metals usage similar to W, Mo, invar with CTE value close to ceramics as the interlayer, can reduce the residual stress. Usage of hard materials with high yield stress as an interlayer is not obviously valid. (4) Using a composite interlayers constituting hard and soft metals like Cu/Mo, Cu/Nb have considerably reduced the residual stress combining the benefits of both type of materials. (5) Joining at the low temperature when joining at that temperature is beneficial for reducing the deformation in the joints and also alleviating the residual stresses. (6) A proper heat treatment after joining releases the residual stresses. (7) Appropriate joint configuration can also reduce the residual stress and stress concentration.

### 7.2 Interface Reliability of the Joints

Interfaces play an important role in determining the properties of joints. Interface property is determined by the interface structure, bonding mechanisms, processing conditions and the materials involved in the joining process. In the presence of charge transfer and no mass transfer through the interface, the bonding is termed as chemical bonding. In case there is mass transfer across the interface in the presence of chemical reaction and diffusion, the bonding mechanism is termed as chemical reaction bonding [60].

#### 7.2.1 Chemical Bonding

Heterogeneous interface among two different types of materials can alter the chemical bonding that can result in different and new properties [61]. Chemical bonding is significantly important in any joining technique and consists of a chemical bond created between both materials through chemical reactions occurring at the metal–ceramic interface. The driving

**Table 3**  $\gamma_{sl}$  values for alumina-metal systems [59]

System	$\gamma_{sl}$ (J/m <sup>2</sup> )	$T_m$ of metal (°C)
Al <sub>2</sub> O <sub>3</sub> –Ag	1.57 at 700 °C	960
Al <sub>2</sub> O <sub>3</sub> –Au	1.80 at 1000 °C	1063
Al <sub>2</sub> O <sub>3</sub> –Cu	2.21 at 900 °C	1083
Al <sub>2</sub> O <sub>3</sub> –Ni	2.20 at 1000 °C	1453
Al <sub>2</sub> O <sub>3</sub> –Fe	2.73 at 1000 °C	1536

force and free energy change for the interface formation have been already discussed in previous Eqs. 5 and 7.

Below Table 3 [59] gives the  $\gamma_{sl}$  values for alumina-metal systems and the value of  $\gamma_{sl}$  is observed to improve with the cohesive energy of the metal which is directly dependent on the melting point of the metal.

### 7.2.2 Chemical Reaction Bonding

In the case of a mass transfer through the interface, the bonds between metal and ceramic are formed by chemical reactions or diffusion. At the interface, the reactions result in the formation of interfacial layers which has properties different from the base material i.e. ceramic and metal [60]. These reactions can have a favorable effect on the quality of the joint produced by enhancing the wettability of metal on the ceramic surface. A thick reaction layer increases the stresses caused by volume mismatch and thermal residual stress which is unfavorable to the joint strength. The reaction is caused when the atomic species diffuse to metal and ceramic side and the driving force for these atomic movements is the chemical potential of the atomic species taking part in the reaction. In various metal–ceramic system, the reaction is not anticipated due to non-interaction of metal and nonmetallic ceramic elements. When the net reaction potentials of the overall species are considered, a net negative free energy may result which implicate the possibility of a possible chemical reaction. Here, equilibrium thermodynamics of the overall system and the species involved can be used to predict the possible reactions. However, the extent of the possible reaction is limited by the kinetic aspects of the system in consideration, the data for which is not readily available for many such metal–ceramic interfaces [62]. Interfacial reaction products like brittle intermetallic and solid solutions cause the interface to rupture at very low stresses. A higher bonding temperature and time lead to the formation of a thick reaction layer which tends to lower the joint strength.

The thickness of such reaction layers is optimized by controlling the bonding parameters in order to prevent the interfacial de-bonding and fracture along with the brittle intermetallic phase. It is observed that the reaction products tend to bond to ceramic with a coherent interface [60].

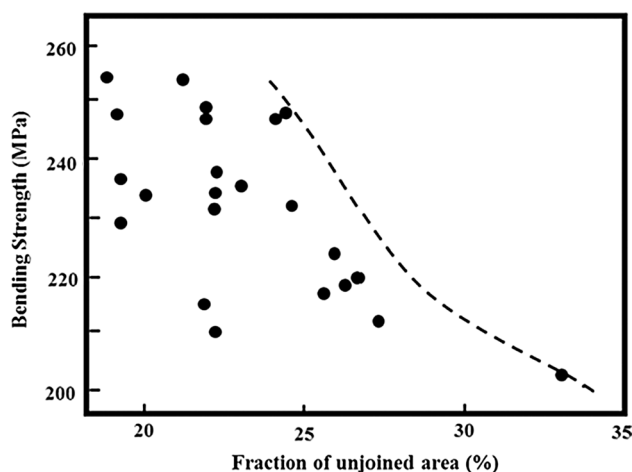


**Fig. 15** Bending strength of individual Al<sub>2</sub>O<sub>3</sub>/Nb joints as a function of unjoined area formed on interface [64]

### 7.2.3 Pores and Un-Bonded Areas on the Interface and Spreadability

The unbonded region at the edges are very common and if not prevented, it acts as a notch and weakens the joint severely due to stress concentration. The pores may as voids or impurity segregation point and degrade the wetting. Therefore, porosity is needed to be controlled for better spreadability and joint strength. In case if the reaction occurring at the interface has gas as one of the reaction products, the interface may be left with pores as a result of gas escape and thus bringing the impediments to the contact. One such case is a Si<sub>3</sub>N<sub>4</sub>/Ni. The interface is weakened due to the presence of pores in the vicinity of the interface. In case if the Ni contains a carbide forming element like Cr, porosity is eliminated, and the strength improves [63, 64]. In a real joining process, impeccable interface connection over the entire surface is rarely achieved for a certain duration of time and temperature and is restricted by the interface reaction. The surface roughness of the base material and the applied pressure most importantly affect the interfacial contact in solid-state bonding [63]. The fracture stress decreases as the unjoined area of the metal–ceramic interface increases and is evident from the below-mentioned Fig. 15. Bending strength of individual Al<sub>2</sub>O<sub>3</sub>–Nb as a function of the unjoined area formed on the interface [64].

## 8 Future Prospects and Conclusions

The phenomenon of wetting, spreading and adhesion from their governing scientific principles and relevance to metal–ceramic joints have been discussed. It's been shown how the presence of an active element in the filler metal

causes reaction with the ceramic to form reaction products which enhance the wetting phenomenon.

Residual and thermal stresses are induced into the joint when it is cooled from brazing temperature to room temperature because of the difference in CTE values of metal–ceramic and is the principal reliability issue and cause of the failure of the joint.

The defects, pores in the bulk and the unbonded regions on metal–ceramic interface raises the stress intensity and act as a site for crack initiation.

The chemical bonding and the extent of reaction at the interface also determine the strength of the joint. A thick layer causes more stress due to volume mismatch and thermal residual stress which further weakens the joint. Hence, a thin reaction layer is desirable which is directly influenced and can be controlled by joining temperature and time.

The current and future work will be oriented towards minimizing the difference in CTE values of metal and ceramic by introducing ceramic particles or use of high entropy filler metal to avoid the growth of brittle intermetallic compounds for good reliability of the joints.

**Acknowledgements** This work was supported by the Technology development program (S2517123) funded by the Ministry of SME's and Startups (MSS, Korea) and also supported by the Korea Institute of Energy Technology Evaluation and Planning (KETEP) and the Ministry of Trade, Industry & Energy (MOTIE) of the Republic of Korea (No. 20172020109280).

## References

- R.W. Davidge, *Contemp. Phys.* **10**, 105 (1969)
- K.J. Kurzydłowski, *Acta Phys. Pol.*, A **96**, 69 (1999)
- W. Fu, X.G. Song, S.P. Hu, J.H. Chai, J.C. Feng, G.D. Wang, *Mater. Des.* **87**, 579 (2015)
- R.W. Messler Jr., *Joining and Materials and Structures*, 1st edn. (Butterworth-Heinemann, New York, 2004)
- A.M. Hadian, *Joining of Silicon Nitride-to-Silicon Nitride and to Molybdenum for High-Temperature Applications*, Ph.D. thesis (McGill University, Montreal, Canada, 1993)
- S.H. Kee, Z. Xu, J.P. Jung, W. Kim, *J. Microelectron. Packag. Soc.* **18**, 1 (2011)
- A. Sharma, S.H. Lee, H.O. Ban, Y.S. Shin, J.P. Jung, *JWJ* **34**, 30 (2016)
- J. Shin, A. Sharma, D.H. Jung, J.P. Jung, *Kor. J. Met. Mater.* **56**, 366 (2018)
- F. Moret, N. Eustathopoulos, *Le Journal de Physique* **IV03(C 7)**, 1043 (1993)
- A. Sharma, S.H. Kee, F. Jung, Y. Heo, J.P. Jung, *J. Mater. Eng. Perform.* **25**(5), 1722 (2016)
- Q. David, *Annu. Rev. Mater. Res.* **38**, 71 (2008)
- D. Bonn, J. Eggers, J. Indekeu, J. Meunier, E. Rolley, *Rev. Mod. Phys.* **81**, 739 (2009)
- E. Thormann, *Curr. Opin. Colloid Interface Sci.* **27**, 18 (2017)
- R.N. Wenzel, *Ind. Eng. Chem.* **28**, 988 (1936)
- C.G.L. Furmidge, *J. Colloid Sci.* **17**, 309 (1962)
- Y. Si, Z. Guo, *Nanoscale* **7**, 5922 (2015)
- A. Adamson, A. Gast, *Physical Chemistry of Surfaces*, 6th edn. (Wiley-Interscience, New York, 1997)
- P.G.D. Gennes, F.B. Wyart, D. Quéré, *Capillarity and Wetting Phenomena*, 1st edn. (Springer-Verlag, New York, 2013)
- P.R. Chidambaram, G.R. Edwards, D.L. Olson, *Metall. Mater. Trans. A* **25**, 2083 (1994)
- P.R. Chidambaram, G.R. Edwards, D.L. Olson, *Metall. Trans. B* **23**, 215 (1992)
- A. Sharma, M.H. Roh, D.H. Jung, J.P. Jung, *Metall. Mater. Trans. A* **47A**, 510 (2016)
- A. Sharma, D.U. Lim, J.P. Jung, *Mater. Sci. Technol.* **32**(8), 773 (2016)
- A. Sharma, M.H. Roh, J.P. Jung, *J. Mater. Eng. Perform.* **25**(8), 3538 (2016)
- A. Sharma, X. Di, J.P. Jung, *Mater. Res. Exp.* **6**(5), 056526 (2019)
- A. Sharma, B.G. Baek, J.P. Jung, *Mater. Des.* **87**, 370 (2015)
- A. Sharma, H. Yu, I.S. Cho, H. Seo, B. Ahn, *Electron. Mater. Lett.* **15**, 27 (2019)
- A. Sharma, A.K. Srivastava, K. Lee, B. Ahn, *Met. Mater. Int.* **25**, 1027 (2019)
- A. Sharma, A.K. Srivastava, B. Ahn, *Mater. Res. Exp.* **6**, 056520 (2019)
- A. Sharma, H.R. Sohn, J.P. Jung, *Metall. Mater. Trans. A* **47**(1), 494 (2016)
- N. Eustathopoulos, M.G. Nicholas, B. Drevet, *Wettability at High Temperatures*, 1st edn. (Pergamon, Oxford, 1999)
- R. Arroyave, *Thermodynamics and Kinetics of Ceramic/Metal Interfacial Interactions* (Ph.D. Thesis, MIT, USA, 2004)
- J.W. Park, P.F. Mendez, T.W. Eagar, *Acta Mater.* **50**, 883 (2002)
- J.A. Fernie, R.A.L. Drew, K.M. Knowles, *Int. Mater. Rev.* **54**, 283 (2009)
- S.H. Kee, S.Y. Park, Y.K. Huh, J.P. Jung, W.J. Kim, *J. Kor. Acad. Prosthodont.* **50**(3), 169 (2012)
- Y.V. Naidich, V.S. Zhuravlev, I.I. Gab, B.D. Kostyuk, V.P. Kravovskyy, A.A. Adamovskyy, NYu. Taranets, *J. Eur. Ceram. Soc.* **28**, 717 (2008)
- O. Dezellus, R. Arroyave, S.G. Fries, *Int. J. Mater. Res.* **102**, 286 (2011)
- R.E. Loehman, A.P. Tomsia, *Acta Metall. Mater.* **40**, S75 (1992)
- R. Voytovych, F. Robaut, N. Eustathopoulos, *Acta Mater.* **54**, 2205 (2006)
- N.Y. Taranets, H. Jones, *Mater. Sci. Eng., A* **379**, 251 (2004)
- V.N. Eremenko, Y.I. Buyanov, N.M. Panchenko, *Sov. Powder Metall. Met. Ceram.* **9**, 410 (1970)
- V.N. Eremenko, Y.I. Buyanov, N.M. Panchenko, *Sov. Powder Metall. Met. Ceram.* **9**, 310 (1970)
- V.N. Eremenko, Y.I. Buyanov, N.M. Panchenko, *Izvestiya Akademii Nauk SSSR, Metall.* **3**, 188 (1969)
- Y. Chang, D. Goldberg, J. Neumann, *J. Phys. Chem.* **6**, 621 (1977)
- O. Kubaschewski, J. De Keyser, R. Schmid-Fetzer, O. Shcherban, V. Tomashik, Y. Jialin, L. Tretyachenko, *Silver-Copper-Titanium*, vol. 11 (Springer, Berlin, 2007), pp. 63–74
- K.T. Raić, *Ceram. Int.* **26**, 19 (2000)
- G. Elssner, G. Petzow, *ISIJ Int.* **30**, 1011 (1990)
- S. Somiya, *Handbook of Advanced Ceramics: Materials, Applications, Processing, and Properties*, 2nd edn. (Academic Press, Cambridge, 2013)
- J. Lemus-Ruiz, L. Ceja-Cárdenas, J.A. Verduzco, O. Flores, *J. Mater. Sci.* **43**, 6296 (2008)
- K. Suganuma, *ISIJ Int.* **30**, 1046 (1990)
- K.A. Khor, M. Wang, W. Zhou, F. Boey, T.S. Srivatsan, *Processing and Fabrication of Advanced Materials VIII* (World Scientific, Singapore, 2001)
- R. Anderson, *Adv. Mater. Processes* **135**, 31 (1989)
- H. Mizuhara, E. Huebel, O.T. Oyama, *Am. Ceram. Soc. Bull.* **68**, 1591 (1989)

53. J. Olofsson, Friction and Wear Mechanisms of Ceramic Surfaces: With Applications to Micro Motors and Hip Joint Replacements (Ph.D. thesis, Uppsala University, Sweden, 2011)
54. B. Çelik B, Thermally Induced Distortion and Residual Stresses in Welded Joints (M.S. thesis, Cukurova University, Turkey, 2009)
55. Y. Zhou, *Microjoining and Nanojoining*, 1st edn. (Elsevier, Amsterdam, 2008)
56. M.B. Uday, M.N. Ahmad Fauzi, H. Zuhailawati, A.B. Ismail, *Mater. Sci. Eng., A* **528**, 4753 (2011)
57. A. Bellosi, T. Kosmac, A.P. Tomsia, *Interfacial Science in Ceramic Joining, Series: Nato Science Partnership Subseries: 3*, vol. 58 (Springer, Berlin, 1998)
58. A.M. Hadian, Joining of Silicon Nitride to Silicon Nitride and to Molybdenum for High Temperature Applications (Ph.D. thesis, McGill University, Montreal, Canada, 1993)
59. R.J. Lemus, Diffusion Bonding of Silicon Nitride to Titanium (Ph.D. thesis, McGill University, Montréal, Canada, 2000)
60. J.W. Park, A Framework for Designing Interlayers for Ceramic to Metal Joints (Ph.D. thesis, Massachusetts Institute of Technology, USA, 2000)
61. W. Wunderlich, *Metals* **4**, 410 (2014)
62. R.M.D. Nascimento, A.E. Martinelli, A.J.A. Buschinelli, *Ceramica* **49**, 178 (2003)
63. M.R. Abbas, M.B. Uday, A.M. Noor, N. Ahmad, Srithar Rajoo, *Mater. Des.* **109**, 47 (2016)
64. K. Suganuma, Reliability Factors in Ceramic/Metal Joining, National Defense Academy Yokosuka, Japan (1993)

**Publisher's Note** Springer Nature remains neutral with regard to jurisdictional claims in published maps and institutional affiliations.